RSC Advances

ROYAL SOCIETY OF CHEMISTRY

www.rsc.org/advances

RSC Advances

ARTICLE

Water sorption properties of room-temperature ionic liquids over the whole range of water activity and molecular state of water in these media

Received 00th January 20xx,
Accepted 00th January 20xx

DOI: 10.1039/x0xx00000x

www.rsc.org/

A. Dahi,[a,b,c] K. Fatyeyeva,[a,b,c] C. Chappey,[a,b,c] D. Langevin,[a,b,c] S. P. Rogalsky,[d] O. P. Tarasyuk,[d] S. Marais[a,b,c]

The water sorption behavior for various RTILs ([C_4C_1im][BF_4], [C_4C_1im][PF_6], [C_6C_1im][PF_6], [C_4im][DBP], [C_4im][BEHP] and [Et_3HN][CF_3SO_3]) was studied over the whole range of water activity using a continuous gravimetric method. Analysis of the water sorption isotherms using the non-random two-liquid model (NRTL) and the combination of a dual-mode sorption (Henry-clustering) allowed a better understanding of the RTIL-water interactions. It is noticed that the sorption of water by RTILs is mainly controlled by the anion's nature. Anions interact with water molecules by hydrogen bonds that promote the formation of a hydrogen bond network between the water molecules. The water uptake by RTILs increases in the following order (up to 0.8 in the water activity a): [C_6C_1im][PF_6] ≤ [C_4C_1im][PF_6] < [C_4C_1im][BF_4] ≈ [C_4im][BEHP] < [Et_3HN][CF_3SO_3] ≤ [C_4im][DBP]. The [PF_6]-based RTILs show the lowest water uptake (low affinity with water; water-immiscible RTILs), whereas [C_4C_1im][BF_4] and [C_4im][BEHP] and especially [C_4im][DBP] and [Et_3HN][CF_3SO_3] exhibit high water uptake (high affinity with water; water-miscible RTILs). At high activity (a > 0.8), water molecules are aggregated only in water-miscible RTILs (case of [C_4im][DBP] and [Et_3HN][CF_3SO_3]) because of their stronger anion basicity. To complete the sorption study, the molecular state of water dissolved in RTILs was studied by the infrared spectroscopy. The water molecules dissolved in water-immiscible RTIL such as [C_4C_1im][PF_6] are not self-associated independently of the water content and, thus, can be defined as "free" water molecules interacting *via* H-bonding with the anions in the symmetric complex: anion…HOH…anion. On the contrary, the water molecules sorbed in water-miscible RTILs such as [C_4im][DBP] or [Et_3HN][CF_3SO_3] are strongly associated by H-bonds and also with the anions even at the low water activity, and are easily aggregated when the water content reaches the critical concentration at high activity.

Introduction

There is now a growing interest in studying the application areas of room-temperature ionic liquids (RTILs). RTILs have attractive physical and chemical properties[1-4] and several advantages over conventional volatile organic solvents, such as good chemical and thermal stability, excellent solvent properties and high conductivity as they entirely consist of the ions (an organic cation and either an organic or an inorganic anion). RTILs are also characterized by the negligible vapor pressure and wide temperature liquid range as they are generally liquid at the ambient temperature (sometimes even up to 300 °C). They are usually non-flammable, non-explosive, recyclable and not so much expensive to manufacture. Moreover, some RTILs properties such as solvent power, water-miscibility and conductivity can be tailored for the specific application by the judicious selection of cations, anions, and substituents. For example, RTIL with 1-*n*-butyl-3-methylimidazolium cation and [PF_6] anion is immiscible with water, whereas RTIL with the same cation and [BF_4] anion is water soluble. This example represents the "designer solvent" property of RTILs: different ion pairs determine physical and chemical properties of the liquid.

Due to their unique and attractive properties, RTILs are becoming an interesting class of solvents for different chemical applications. RTILs are excellent solvents for organic/inorganic synthesis[1,5,6] and catalysis[6]. Many compounds, both polar and nonpolar, may be dissolved readily in RTILs. Thus, there is the potential in using the RTIL solvents to carry out reactions that are traditionally multiphase (and mass-transfer limited) in a single phase[3]. RTILs are also good solvents for the extraction and purification processes[8]. Many volatile organic solvents used in extraction are known for their flammability, volatility, toxicity and use in large quantities. Therefore, due to their specific properties mentioned above, RTILs represent a potential replacement for these organic solvents. The non-volatility of RTILs allows them to be used in severe temperature and pressure conditions. The use of

[a] Normandie Univ
[b] Université de Rouen, Laboratoire Polymères, Biopolymères, Surfaces, Bd. Maurice de Broglie, 76821 Mont Saint Aignan cedex, France.
[c] UMR 6270 CNRS & FR 3038, 76821 Mont Saint Aignan cedex, France.
[d] Institute of Bioorganic Chemistry and Petrochemistry, National Academy of Sciences of Ukraine, 50, Kharkivske schose, 02160 Kyiv, Ukraine.

RTILs in preparing the separation membranes significantly improves the performance of the resulting materials[9-12]. Several researches have shown that the composite membranes containing RTILs allow selective transport of organic compounds (such as amines[13] and aromatic hydrocarbons[14,15]), vapors[11,16,17] and gases[18,19] , and metal ions[20,21]. Besides, RTILs have a number of properties[22-24] (a wide electrochemical window (> 4 V), a high conductivity, a wide operating temperature range, and a low dielectric constant) that make them attractive for electrochemical applications in batteries and fuel cells[25-27]. This is one of the well-studied application areas for RTILs.

The quite rapid emergence of RTILs as the alternative solvents has resulted in a rapidly growing number of applications and required a better understanding of their physical and chemical properties towards external molecules[2,28]. Some physical and chemical properties of RTILs (such as viscosity, density, conductivity and solvating ability) are very sensitive to impurities, like water[29-35]. Poorly dried RTILs or RTILs exposed to ambient air may contain some amount of water which will affect their performance even at the very small concentrations and, consequently, will cause severe problems for certain applications. For example, the presence of water in RTILs influences the solubility of organic/inorganic substances as well as modifies the rates and selectivity of chemical reactions performed in these media[36]. It is also known that RTILs based on $[PF_6]$ anions tend to form HF in the presence of catalytic quantities of water and acids[1,2,30,37]. The activity of the catalyst in RTIL can decrease in the presence of water[38]. Fortunato et al. evaluated the transport of various amino acids through a supported ionic liquid membrane. The transport mechanism is found to be disrupted because it is mainly regulated by the mobility of water inside RTIL, rather than by the RTIL selectivity towards the solute. For all these moisture sensitive applications, RTILs must be dried before any use (even if they are immiscible with water), and then handled under the inert atmosphere. On the other hand, there are other applications where the contact between RTILs and water is unavoidable and, in some cases, the presence of water is very useful and necessary. Brown et al.[40] studied the asymmetric hydrogenation of tiglic acid catalyzed by $Ru(O_2CMe)_2$((*R*)–tolBINAP) in imidazolium RTIL with the addition of water as cosolvent. Wang et al.[11] showed that the supported liquid membranes based on RTILs can be very promising for separating organic/water mixtures. Fadeev et al.[41] demonstrated that two imidazolium RTILs could be used for the extraction of butanol from aqueous fermentation broths. Visser et al.[42] designed and synthesized several RTILs to remove cadmium and mercury ions from the contaminated water. Fujita et al.[43] indicated that some proteins which are insoluble in RTILs can be solubilized as well as stabilized in the RTIL-water mixtures. Besides, many RTILs were efficiently used for the water vapor removing from gas mixtures[34]. Scovazzo[12] studied the dehumidification of both nitrogen and methane using the supported ionic liquid membranes. Zhao et al.[44] studied the effect of the water content in $[C_4C_1im][BF_4]$ on CO_2/N_2 separation performance of the polyethersulfone supported ionic liquid membrane. A small addition of water in $[C_8C_1im][BF_4]$ improved the performance of the resulting membrane. In short, many processes using RTILs require the presence of water. Therefore, it is necessary to accumulate a substantial body of data on the RTIL-water interactions so that the true potential of RTILs as solvents can be realized. Such data are very helpful as the majority of RTILs are hygroscopic and can absorb significant amounts of water from the atmosphere even being hydrophobic[30,33-35]. Their hygroscopic level depends primary on the nature of their ions (cation and anion), on the relative humidity and the temperature. Cao et al.[45,46]noted the influence of the structural (cation and anion type, as well as cation alkyl chain length) and external (temperature, relative, humidity and the presence of impurities) factors on the water sorption in conventional and functionalized RTILs. Three types of parameters (sorption capacity, sorption rate and sorption equilibrium) derived from the modified two-step sorption mechanism were used for analyzing the water sorption processes in RTILs. Also, a sorption triangle between these parameters was proposed allowing the qualitative analysis of the RTIL water sorption behavior. In its turn, Seddon et al.[29] provided some general guidelines on the effect of anion choice on the miscibility of RTILs in water. They indicate that the imidazolium salts with the halide, ethanoate, acetate, nitrate and trifluoroacetate anions are totally miscible with water, while the $[(CF_3SO_2)_2N]$ and $[PF_6]$ imidazolium salts are immiscible, whereas $[CF_3SO_3]$ and $[BF_4]$ imidazolium salts can be either totally miscible or immiscible depending on the substituents on the cation.

The infrared spectroscopy is extensively used for understanding the interactions between the water molecules and RTILs. The vibrational modes of water are very sensitive to the environment and intermolecular interactions[47,48]. Most of the published studies are devoted to the water-anion and water-cation interactions, to the hydration of RTILs and to the effect of RTIL structure on the water hydrogen bonding environment. Singh et al.[49] examined the cation–anion–water interactions in aqueous mixtures of imidazolium RTILs ($[C_4C_1im][BF_4]$, $[C_8C_1im][Cl]$, $[C_4C_1im][CH_3OSO_3]$ and $[C_4C_1im][C_8H_{17}OSO_3]$) over the whole composition range using FTIR spectroscopy. Andanson et al.[31] investigated the RTIL-water interactions in both $[C_4C_1im][BF_4]$-water and $[C_4C_1im][PF_6]$-water binary systems using attenuated total reflection (ATR) infrared spectroscopy on dry and wet RTILs at 40 °C. The infrared measurement studies of Cammarata et al.[30] demonstrated that the water molecules absorbed by 1-alkyl-3-methylimidazolium RTILs from the air are mostly present in a free (not self-associated) state, bonded *via* H-bonding with the $[PF_6]$, $[BF_4]$, $[SbF_6]$, $[ClO_4]$, $[CF_3SO_3]$ and $[(CF_3SO_2)_2N]$ anions in a symmetric complex: anion...H–O–H...anion. Chen et al. studied the interaction mechanisms between allyl- and amine-functionalized RTILs[46], acetate-based RTILs[50], and water in the whole concentration range by ^1H NMR and ATR-IR measurements. The molecular organization of a small concentration of water diluted in imidazolium RTILs using IR and Raman spectroscopy was also analyzed and compared to the density functional theory (DFT) calculations in order to validate the structure of wet RTILs[51]. Near-infrared spectrometry was used by

Tran et al.[33] for determining the concentration and structure of water absorbed by $[C_4C_1im][BF_4]$, $[C_4C_1im][Tf_2N]$ and $[C_4C_1im][PF_6]$. So, IR spectroscopy demonstrated a great potential for the precise investigation of the molecular interactions in the RTIL-water binary systems. Nevertheless, to our knowledge, very little attention was paid to the RTIL-water interactions in terms of water uptake and water isotherms as well as sorption mathematical models over the whole range of the water activity. Anthony et al.[34] measured the amount of water absorbed by $[C_4C_1im][PF_6]$, $[C_8C_1im][PF_6]$ and $[C_8C_1im][BF_4]$ when exposed to various water vapor pressures. The authors indicate that the affinity to water is greater for RTILs used $[BF_4]$ as the anion than for those used $[PF_6]$, and that the water affinity decreases with increasing the alkyl chain length.

The objective of this work is to gain an understanding of the water sorption behavior of different types of RTILs (1-butyl-3-methylimidazolium tetrafluoroborate ($[C_4C_1im][BF_4]$), 1-butyl-3-methylimidazolium hexafluorophosphate ($[C_4C_1im][PF_6]$), 1-hexyl-3-methylimidazolium hexafluorophosphate ($[C_6C_1im][PF_6]$), 1-n-butylimidazolium dibutylphosphate ($[C_4im][DBP]$), 1-n-butylimidazolium bis(2-ethylhexyl)phosphate ($[C_4im][BEHP]$) and triethylammonium trifluoromethanesulfonate ($[Et_3HN][CF_3SO_3]$)) over the whole range of the water activity. Imidazolium RTILs constitute a large family of anion–cation couples considered as the model systems whose physical and chemical properties are being intensively investigated. In addition, ammonium RTIL ($[Et_3HN][CF_3SO_3]$) is the reference RTIL studied for the electrochemical systems[22,52]. To determine the RTIL water uptake as a function of the water activity, the water vapor sorption measurements were carried out using the gravimetric method. The obtained water sorption isotherms were further adjusted and analyzed by the most appropriate sorption models in order to understand the sorption behavior of water in RTILs. Studied RTILs arouse our interest not only in their good stability and attractive properties[1-4] but also in the fact that they differ in the anion and cation groups and, thus, in the hydrophobic/hydrophilic and protic/aprotic balances. This allowed us to investigate the cation-anion-water interactions and, therefore, to understand the relationship between the structure of RTILs and their water sorption properties. To complete the study of the water sorption behavior in such RTILs, the molecular state of water dissolved in ionic liquids was investigated by the infrared spectroscopy as a function of the water activity.

Experimental

Room-temperature ionic liquids

The chemical structure of RTILs used in the work is shown in **Fig. 1**. $[C_4C_1im][BF_4]$, $[C_4C_1im][PF_6]$ and $[C_6C_1im][PF_6]$ were purchased from Acros Organics (>98% purity) and used as received. $[C_4im][DBP]$ and $[C_4im][BEHP]$ were prepared by mixing the equimolar quantities of 1-*n*-butylimidazole (1) either with dibutylphosphate (2) to obtain $[C_4im][DBP]$, or with bis-(2-ethylhexyl)phosphate (3) to obtain $[C_4im][BEHP]$ (**Fig. 2**). $[Et_3HN][CF_3SO_3]$ was synthesized at the LEPMI

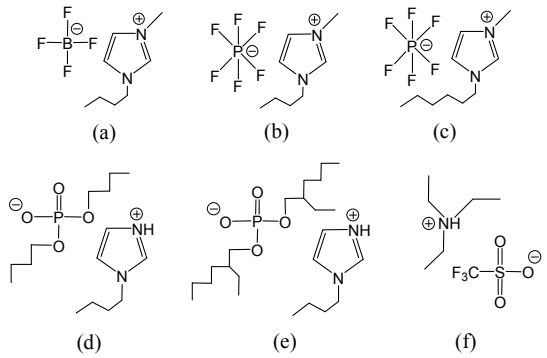

Fig. 1. Chemical structure of studied RTILs: (a) $[C_4C_1im][BF_4]$, (b) $[C_4C_1im][PF_6]$, (c) $[C_6C_1im][PF_6]$, (d) $[C_4im][DBP]$, (e) $[C_4im][BEHP]$ and (f) $[Et_3HN][CF_3SO_3]$.

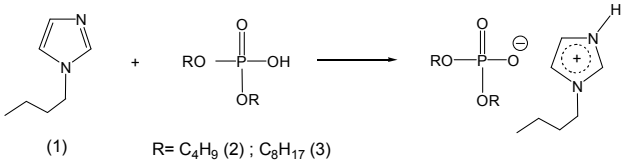

Fig. 2. Reaction scheme of the synthesis of $[C_4im][DBP]$ and $[C_4im][BEHP]$.

Laboratory (UMR 5279 CNRS, France) according to the procedure already described in the separate paper[52].

Sorption studies

The water vapor sorption kinetics measurements were carried out at 25 °C using a continuous gravimetric method. The electronic microbalance used was a microbalance IGAsorp (Intelligent Gravimetric Analyser Sorption moisture) supplied by Hiden Isochema Limited (UK). First, the sample (RTIL) was placed into a sample pan, retained on one end of the electronic microbalance. The sample environment temperature was controlled by the thermoregulated water bath and fixed at 25 °C. The sample was dried by the dry flow of N_2 gas until a constant mass was obtained. Afterwards, the water vapor pressure was increased on different levels up to the saturated vapor pressure. At each step, the water uptake was continuously measured as a function of time until an equilibrium state was reached. The water content at equilibrium was used to build the water vapor sorption isotherm. All water used was milli-Q water (resistivity = 18 MΩ/cm at 25 °C).

Infrared spectroscopy

The IR measurements were carried out by Avatar 360 FTIR spectrometer (Thermo Fisher) using the ATR mode equipped with a diamond crystal. It was shown that single reflection ATR (incident angle 45°) ensured a better detection of the IR bands of the vibrational modes of water dissolved in RTILs[30]. 200 scans were collected for each spectrum over the spectral range 650-4000 cm^{-1} with a resolution of 8 cm^{-1}. All spectra were normalized to a reference peak that was chosen because of its invariability in the course of the water vapor sorption. The reference peak was dependent on RTIL, *i.e.* 814.9 cm^{-1} for $[C_4C_1im][PF_6]$, 1169.7 cm^{-1} for

$[C_4C_1im][BF_4]$, 1400.2 cm^{-1} for $[Et_3HN][CF_3SO_3]$, 1465.7 cm^{-1} for $[C_4im][DBP]$ and 1461.8 cm^{-1} in the case of $[C_4im][BEHP]$.

The IR measurements were performed for RTILs with the different water contents. For each RTIL, an IR spectrum was measured just at the end of the water vapor sorption experiment, *i.e.* RTIL equilibrated at water activity a = 0.95 was studied. In order to place RTIL in the low activity conditions (0 < a < 0.95), RTIL was first dried at 80 °C and then placed in an Eppendorf tube (with a tight fitting lid). Then, using the data of the water vapor sorption isotherm, a precise amount of water was added by a micropipette (Ergonomic High-Performance). This added amount corresponds to a water uptake at a given activity. After the complete absorption of water by RTIL, the IR spectrum was measured.

Results and discussion

Water sorption by RTILs

To understand the key interactions between the water molecules and RTILs, a continuous gravimetric analysis was performed. **Fig. 3** shows the water vapor sorption isotherms of $[C_4C_1im][BF_4]$, $[C_6C_1im][PF_6]$, $[C_4C_1im][PF_6]$, $[C_4im][BEHP]$, $[Et_3HN][CF_3SO_3]$ and $[C_4im][DBP]$. As one can notice, the behavior of the sorption isotherms for all studied RTILs is similar: the mass uptake is linear and non-specific at the low and intermediate water activity (up to a < 0.8) and then it increases exponentially for the high water activity (a > 0.8).

Different models exist to describe the sorption of vapors by liquids (Vapor Liquid Equilibria (VLE)) but the NRTL model remains the most common local-composition model. If we assume that the vapor pressure for RTIL is zero (p_2^{sat} = 0) due to the low volatility of RTILs and consider that the pressures are sufficiently low, the pressure p in the binary mixture water (1)-RTIL (2) can be estimated according to the following equation[16,53]:

$$p = p_1^{sat} \cdot \chi_1 \cdot \gamma_1 \quad (1)$$

where p_1^{sat} is the vapor pressure of the pure water and χ_1 is the mole fraction of water in the liquid phase. γ_1 is the activity coefficient of water that can be determined from:

$$ln\,\gamma_1 = \chi_2^2\left[\tau_{21}\left(\frac{G_{21}}{\chi_1+\chi_2 G_{21}}\right)^2 + \frac{\tau_{12}G_{12}}{(\chi_2+\chi_1 G_{12})^2}\right] \quad (2)$$

with $\ln G_{ij} = -\alpha_{ij}\cdot\tau_{ij}$

The parameters α_{12} and α_{21} are the so-called non-randomness parameters, for which α_{12} is usually set equal to α_{21}. The parameters τ_{12} and τ_{21} are the dimensionless interaction parameters, which are related to the interaction energy parameters Δg_{12} and Δg_{21} by:

$$\tau_{ij} = \frac{\Delta g_{ij}}{RT} = \frac{(g_{ij} - g_{jj})}{RT} \quad (3)$$

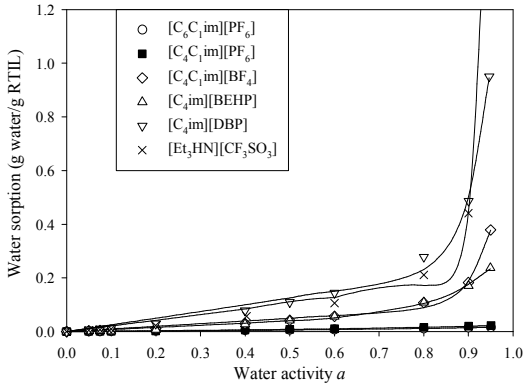

Fig. 3. Water vapor sorption isotherms of $[C_6C_1im][PF_6]$, $[C_4C_1im][PF_6]$, $[C_4C_1im][BF_4]$, $[C_4im][BEHP]$, $[C_4im][DBP]$ and $[Et_3HN][CF_3SO_3]$ at 25 °C. Data were fit with the Henry-clustering equation.

where R is the gas constant and T is the absolute temperature, and g_{ij} is the energy parameter characteristic of the *i-j* interaction.

The constants of the NRTL model (α_{12}, τ_{12} and τ_{21}) are empirical since they were determined by fit to experimental data of p (determined from the water sorption data) as a function of the mole fraction of water (using Table curve 2D software) and are listed in **Table 1**.

The comparison of the experimental and predicted VLE curves (**Fig. 4**) reveals a good concordance of the NRTL model with the water vapor sorption in the case of $[C_6C_1im][PF_6]$, $[C_4C_1im][PF_6]$ and $[C_4C_1im][BF_4]$. However, some deviation of the experimental results from those predicted by the NRTL model is observed in the case of $[C_4im][DBP]$, $[C_4im][BEHP]$ and $[Et_3HN][CF_3SO_3]$. Depending on the binary system, the values of the α constant are found to be 0.2 for $[PF_6]$-RTIL and $[C_4im][DBP]$, and 0.5 for $[C_4C_1im][BF_4]$, $[C_4im][BEHP]$ and $[Et_3HN][CF_3SO_3]$ (**Table 1**). Keeping in mind that for a large number of the binary systems the α constant varies from 0.2 to 0.47 and that in the ideal case of the random system α is equal to 0, the highest value of α (0.5) means that the water molecules are less randomly dispersed in $[C_4C_1im][BF_4]$, $[C_4im][BEHP]$ and $[Et_3HN][CF_3SO_3]$. The τ values can be interpreted in terms of the differences in the interaction energies between the solute molecule and RTIL. The cation/anion interaction should be the strongest one, followed by the anion/solvent and cation/solvent interactions, and the solvent/solvent interactions should be the weakest. This means that one would expect: $\tau_{21} \le 0$; $\tau_{12} \ge 0$; $|\tau_{21}| << |\tau_{12}|$[54] (index 1 respectively corresponds to the solute and index 2 – to RTIL). From **Table 1**, this supposition is confirmed only in the case of $[C_6C_1im][PF_6]$, $[C_4C_1im][PF_6]$ and $[C_4C_1im][BF_4]$, which belong to the family of 1,3-dialkylimidazolium based ionic liquids. This result agrees with the works of Revelli et al.[53] who studied (vapor + liquid) equilibrium of the binary mixtures containing methanol or ethanol and three RTILs based on 1,3-dialkylimidazolium ($[C_4C_1im][BF_4]$, $[C_4C_1im][HSO_4]$ and $[C_4C_1im][CH_3COO]$). They showed that the NRTL model can be applied successfully to such systems.

For a better understanding of the water behavior in RTILs and in addition to the NRTL model, the sorption data were also analyzed

Table 1. Binary NRTL parameters of water vapor in RTILs at 25 °C.

RTIL	α^{*}_{12}	τ_{12}	τ_{21}
$[C_6C_1im][PF_6]$	0.2	3.57	0.15
$[C_4C_1im][PF_6]$	0.2	5.61	-0.29
$[C_4C_1im][BF_4]$	0.5	2.77	-0.31
$[C_4im][BEHP]$	0.5	-0.65	1.31
$[C_4im][DBP]$	0.2	1.84	-2.25
$[Et_3HN][TfO]$	0.5	-0.96	1.35

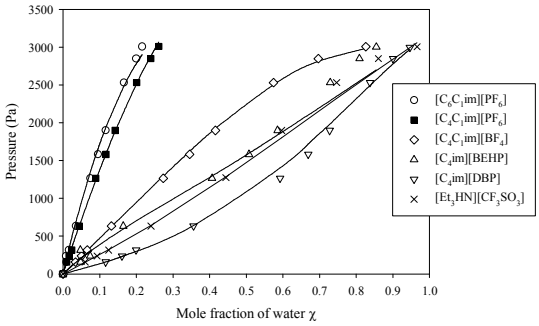

*1 - solute, 2 - RTIL

Fig. 4. Experimental and calculated partial pressure versus mole fraction according to the NRTL model for the binary system (at 25 °C): water + RTIL.

by the other approach using a mechanistic insight into the sorption isotherms. As shown in **Fig. 3**, the shape of all sorption isotherm curves exhibits a linear part at the water activity lower than 0.7 followed by an upward curvature for the higher activity. This convex shape is usually described by the sorption of type III according to Rogers's classification or BET III. In this case, the most cited model is Flory-Huggins[554] usually applied for the non-polar solvents. In the case of the polar solvents, and especially for water, the exponential increase of the mass gain is usually explained by the water molecule aggregation. The study of Anthony et al.[34] indicates that the water solubility in RTILs is linear at the lowest activities according to the Henry's law. Cao et al.[45] in the performed research on the water sorption of RTILs at the constant relative humidity of 52 % also proposed the models based on the water molecule adsorption on the RTIL surface (Langmuir's sorption) and on the water molecule absorption into the RTIL bulk according to the Henry's law. As in our case the Langmuir's sorption mode is absent (see **Fig. 3**), therefore, for the modelling of the water sorption by RTILs, it is logically to consider the combination of two sorption modes, Henry and clustering, in the whole range of the water activity. The equation of the dual mode sorption Henry-clustering (Eq. 4) has been derived from the Park model[56] used for the sorption isotherms of the hydrophilic polymers by removing the Langmuir contribution (not present here). In this case, it is assumed that two species of the sorbed molecules contribute to the apparent water concentration in the sample. One of these species follows the Henry's law at the low water activity and the other one follows the water clustering at high activity:

(4)

where C_{H_2O} (g-water/g-RTIL) is the water concentration, and $C_{(H_2O)_D}$ and ($n \cdot C_{(H_2O)_n}$) are the concentration of Henry's law species and the aggregated species, respectively; *a* is the activity, k_D (g-water/g-RTIL) is the Henry's solubility coefficient representing the affinity of the water molecules to the sorbent sample, *n* is the mean number of the water molecules per cluster, and K_a ((g-water/g-RTIL)$^{1-n}$) is the equilibrium constant for the clustering reaction. The constants of the Henry-clustering equation (k_D, K_a and *n*) were obtained by fitting the experimental data and are listed in **Table 2.**

Fig. 3 shows that the RTIL water uptake is low at the low water activity. Thus, the interactions between the water and RTILs are weak at the low water concentration. The water uptake increases progressively and linearly with the water activity ($C_{H_2O} = k_D \cdot a$; no aggregation at the low and intermediate activity). This linear increase depends only on the Henry's solubility coefficient (k_D) (the slope of the curve) reflecting the affinity between the water molecules and each RTIL. The higher the k_D value, the higher the amount of water absorbed by RTIL. The water uptake increases in the following order (up to a = 0.8): $[C_6C_1im][PF_6]$ ≤ $[C_4C_1im][PF_6]$ < $[C_4C_1im][BF_4]$ ≈ $[C_4im][BEHP]$ < $[Et_3HN][CF_3SO_3]$ ≤ $[C_4im][DBP]$ (**Fig. 3**). $[C_6C_1im][PF_6]$ and $[C_4C_1im][PF_6]$ show the lowest water uptake, and consequently the lowest k_D values (**Table 2**). The water molecules have therefore a very low affinity for these two RTILs, which confirms their hydrophobic character due to $[PF_6]$. The k_D values for $[C_4C_1im][BF_4]$ and $[C_4im][BEHP]$ are the magnitude of the same order, but are higher compared with those for $[C_4C_1im][PF_6]$ and $[C_6C_1im][PF_6]$ (**Table 2**). As it can be observed in **Fig. 3**, the amount of water absorbed by $[C_4C_1im][BF_4]$ or $[C_4im][BEHP]$ is always higher than that absorbed by $[C_4C_1im][PF_6]$ and $[C_6C_1im][PF_6]$ and this difference is more pronounced at the higher water activity. One can say that the water molecules have more affinity or strong interactions with $[C_4C_1im][BF_4]$ and $[C_4im][BEHP]$ than with $[C_4C_1im][PF_6]$ and $[C_6C_1im][PF_6]$. The same takes place for $[C_4im][DBP]$ and $[Et_3HN][CF_3SO_3]$ that show the strongest water uptakes (**Fig. 3**) and, thus, the highest k_D values (**Table 2**). Thereby, their interactions with the water molecules are stronger than those for other studied RTILs. It is interesting to note that the different RTILs ($[C_4C_1im][BF_4]$ and$[C_4im][BEHP]$ as well as $[C_4im][DBP]$ and $[Et_3HN][CF_3SO_3]$) present almost the same interactions with the water molecules (*i.e.* the similar water vapor sorption isotherms up to a = 0.8 and thus the similar values of k_D), although their chemical structures are different (**Fig. 1**). The experimental data overlap even in the case of the pair $[C_4C_1im][BF_4]$-$[C_4im][BEHP]$.

At the high activity (a > 0.8), the exponential increase in the water uptake reveals the water clustering formation which occurs in $[C_4C_1im][BF_4]$, $[C_4im][BEHP]$, $[C_4im][DBP]$ and especially in the case of $[Et_3HN][CF_3SO_3]$. Consequently, the values of K_a (the equilibrium constant for the clustering reaction) and n (the mean number of the water molecules per cluster) for these RTILs are higher in comparison with those for $[C_4C_1im][PF_6]$ and $[C_6C_1im][PF_6]$ (**Table 2**). The aggregation process is clearly linked to the affinity between the water molecules and RTIL. As it was noted above, the affinities or interactions with water are very low in the case of hydrophobic $[PF_6]$-based RTILs. This fact explains why the water molecules are aggregated very weakly in $[C_4C_1im][PF_6]$ and $[C_6C_1im][PF_6]$ at the high activity. Fortunato et al.[10,39] studied the water uptake of imidazolium-based RTILs ($[C_nC_1im][PF_6]$ with n = 4, 8 and 10 and $[C_nC_1im][BF_4]$ with n= 4 and 10) after the contact with the aqueous solutions. They concluded that the water molecules began to cluster on the molecular level after the water content in RTIL exceeded a critical concentration. According to Scovazzo et al.[12], the critical concentration for the water cluster formation is an anion dependent and higher and easier to reach for the water-miscible RTILs compared to the water-immiscible RTILs. Combining our results with the studies of Fortunato et al.[10,39] and Scovazzo et al.[12], it can be stated that $[C_4C_1im][PF_6]$ and $[C_6C_1im][PF_6]$ are water-immiscible RTILs, while $[C_4C_1im][BF_4]$, $[C_4im][BEHP]$, $[C_4im][DBP]$ and $[Et_3HN][CF_3SO_3]$ are water-miscible RTILs. On the other hand, one can see that the RTIL's pairs $[C_4C_1im][BF_4]$-$[C_4im][BEHP]$ and $[C_4im][DBP]$-$[Et_3HN][CF_3SO_3]$ show almost the same sorption behavior towards the water molecules at the low and intermediate activity. On the contrary, their water vapor sorption isotherms are not similar at a > 0.85 (**Fig. 3**), *i.e.* the water molecules are aggregated differently in each RTIL. For the first pair ($[C_4C_1im][BF_4]$-$[C_4im][BEHP]$), the K_a value in the case of $[C_4C_1im][BF_4]$ is much higher than that found for $[C_4im][BEHP]$ (**Table 2**). The water molecules therefore are aggregated more easily in $[C_4C_1im][BF_4]$ than in $[C_4im][BEHP]$. The same reflection may be applied to the second pair ($[C_4im][DBP]$-$[Et_3HN][CF_3SO_3]$): $[Et_3HN][CF_3SO_3]$ shows the highest values of K_a and n (**Table 2**), which are totally different from those obtained for $[C_4im][DBP]$. The obtained results show that $[Et_3HN][CF_3SO_3]$ absorbs twice its dry mass (2.03 g-water/g-RTIL) at a = 0.95 (not visible in **Fig. 3**), while $[C_4im][DBP]$ absorbs only its dry mass (0.95 g-water/g-RTIL) (**Fig. 3**). Therefore, the behavior of two RTILs towards the water molecules can be similar at the given activity value and very different at the other activity value. This can be illustrated by comparing $[C_4im][DBP]$ and $[Et_3HN][CF_3SO_3]$ along the entire activity scale (**Fig. 3**). Indeed, water is slightly more soluble in $[C_4im][DBP]$ than in $[Et_3HN][CF_3SO_3]$ at the intermediate water activity (compare their k_D values (**Table 2**)), but at the high activity the water aggregation is very important in $[Et_3HN][CF_3SO_3]$ compared to $[C_4im][DBP]$ (see their K_a values (**Table 2**)). The sorption isotherms of these two RTILs reveal an overlapping at a = 0.9. The comparison of $[C_4C_1im][BF_4]$ and $[C_4im][DBP]$ is also of interest. Although the water uptake is high in $[C_4im][DBP]$ along the entire activity scale (the k_D value is higher for $[C_4im][DBP]$ than for $[C_4C_1im][BF_4]$ (**Table 2**)), the water molecules appear to be aggregated more easily in $[C_4C_1im][BF_4]$ than in $[C_4im][DBP]$ (compare their values of K_a and n (**Table 2**)).

Table 2. Henry-clustering sorption parameters of water vapor in RTILs at 25 °C.

Constants	$[C_4C_1im][PF_6]$	$[C_6C_1im][PF_6]$	$[C_4C_1im][BF_4]$	$[C_4im][BEHP]$	$[C_4im][DBP]$	$[Et_3HN][CF_3SO_3]$
k_D (g-water/g-RTIL)	$1.5 \cdot 10^{-2}$	$1.1 \cdot 10^{-2}$	$9.8 \cdot 10^{-2}$	$7.8 \cdot 10^{-2}$	$25.0 \cdot 10^{-2}$	$21.1 \cdot 10^{-2}$
K_a ((g-water/g-RTIL)$^{1-n}$)	$7.5 \cdot 10^{4}$	$1.2 \cdot 10^{4}$	$1.2 \cdot 10^{18}$	$1.1 \cdot 10^{7}$	$1.7 \cdot 10^{10}$	$3.4 \cdot 10^{24}$
n (-)	4.1	3.5	19.3	7.7	18.6	37.0

All these results are in good agreement with the literature which qualifies $[C_4C_1im][BF_4]$[1,2,30,31,33,57], $[C_4im][DBP]$[58-60] and $[Et_3HN][CF_3SO_3]$[57] RTILs as miscible with water, while $[C_4C_1im][PF_6]$ and $[C_6C_1im][PF_6]$ are water-immiscible[1,2,30,31,33,57]. For $[C_4im][BEHP]$, few literature data are available on the water uptake. RTILs with the alkyl-substituted imidazolium cation and dialkylphosphate anion, like $[C_4im][BEHP]$ and $[C_4im][DBP]$, are often qualified as hydrophilic RTILs[60-62]. The water sorption capacity of RTILs depends on the nature of RTILs, the relative humidity and the temperature. According to several researchers[29-31,33,34,49,57], the anion plays a main part in the water sorption by RTILs. It interacts with water by the hydrogen bonds but also it can promote the formation of a hydrogen bond network between the water molecules. All these hydrogen bonding interactions are responsible for the water sorption in RTILs[29-3&,33,49] and the strength of these interactions depends primarily on the anion. The $[BF_4]$ anion, compared to $[PF_6]$ one, promotes the strong hydrogen bonds with and between the water molecules[30,31,33,49], which are explained by both the strong water uptake and the formation of the water aggregates in $[C_4C_1im][BF_4]$, compared to $[C_4C_1im][PF_6]$ (**Fig. 3**). The different behavior of the $[BF_4]$ and $[PF_6]$ anions is attributed to the fact that the $[BF_4]$ van der Waals volume (48 Å^3) is smaller than the $[PF_6]$ one (68 Å^3), that gives more space for the water molecules to accommodate in $[BF_4]$-based RTILs[10,34]. Jureviciute et al.[63] suppose that water is more soluble in the systems where the counter-anion is $[BF_4]$ rather than $[PF_6]$, since the $[BF_4]$ anion is smaller allowing more free volume for the water molecules. This idea is also in accordance with the study of Tran et al.[33] showing that $[C_4C_1im][PF_6]$, $[C_4C_1im][Tf_2N]$ and $[C_4C_1im][BF_4]$ after being exposed to air for 24 h can absorb up to 0.083, 0.097 and 0.32 M of water, respectively. The $[DBP]$ and $[BEHP]$ anions reveal the same behavior. The lengthening and the branching of the alkyl side-chains on the anion (*i.e.* from $[C_4im][DBP]$ to $[C_4im][BEHP]$) leads to a significant decrease of both the water uptake and the water aggregation. This is most likely due to the increase of the

hydrophobic character of RTIL and to the steric hindrance of the anion-water interactions[16]. To our knowledge, no data on the water sorption in $[C_4im][BEHP]$ and $[C_4im][DBP]$ are available in the literature.

The effect of the cation on the water sorption in RTILs is not negligible, but remains secondary compared to that of the anion[1,2,30,33]. For example, Cao et al.[45] studied the effects of the IL structural factors (type of cation and anion, alkyl chain length at cation and C2 methylation at cation) on the water sorption kinetics for several RTILs. They revealed that RTILs with large elongated cations led to weaker interactions with water compared to those with small ions because of the ion charge delocalization. In addition, they came to the conclusion about the dominating influence of the anion on the water sorption. The protic RTILs, $[C_4im][BEHP]$ and especially $[C_4im][DBP]$ and $[Et_3HN][CF_3SO_3]$, show the high water uptake. Their protonated cations appear to interact with the water molecules by the hydrogen bonds and consequently participate in the formation of the hydrogen bond network. These cation-water interactions promote the water uptake and water aggregation in these protic RTILs, but remain weak compared to the anion-water interactions. Finally, in $[C_nC_1im][PF_6]$ (n = 4 or 6), the water uptake decreases with growing number of carbon probably due to the increase of the hydrophobic character of RTIL and also to the steric hindrance of the anion-water interactions[16]. In literature, it was already mentioned that the hydrophobicity of RTILs increased with the alkyl chain length increase[45].

The obtained results show that the amount of water sorbed in RTILs increases in the following orders $[PF_6] < [BF_4] \approx [BEHP] < [DBP] < [CF_3SO_3]$ (for the same cation) and $[C_6C_1im] \leq [C_4C_1im] \leq [C_4im] < [Et_3HN]$ (for the same anion). This result is in agreement with the data available in the literature[30,31,33,49,57]. Moreover, the water sorption in studied RTILs seems to be governed by the same mechanism, mainly by the association of the two sorption modes – Henry and clustering.

Molecular states of water in RTILs

The question arises whether the molecular state of water dissolved in RTILs is strongly influenced by its concentration. We are interested in the molecular state of water based on the positions of the water characteristic IR bands. Each RTIL was equilibrated at various activity levels according to the experimental sorption isotherms.

The IR band corresponding to the bending mode (ν_2) of water (either pure or dissolved in solvents) is usually located in the region of 1595 - 1650 cm^{-1}, and is rarely used to clarify the water molecular state[30,31,49]. On the contrary, stretching vibration modes of water are widely used to study the molecular state of water dissolved in various solvents and absorbed in different materials[64,65]. The IR bands appeared in the region of 3000 - 3800 cm^{-1} correspond to the antisymmetric (ν_3) and symmetric (ν_1) stretching modes. Their position and intensity are very sensitive to the water environment and to the water association *via* H-bonding. In the water vapor, the ν_3 and ν_1 bands present at 3756 and 3657 cm^{-1}, respectively. In this case, the water molecules are distant from each other, they are not associated with each other by the hydrogen bonds and, consequently, remain free. In the IR spectrum of the liquid water, the presence of H-bonding is characterized by the overlapping of the ν_3 and ν_1 bands leading to a broad and intense band with a maximum at around 3300 cm^{-1}. It is also important to note that the ν_3 and ν_1 bands shift to the lower wavenumber region when water interacts with the environment (*e.g.* water dissolved in a solvent or sorbed into a polymer).

Figures 5 to 9 show the normalized ATR-FTIR spectra of prehydrated RTILs - $[C_4C_1im][PF_6]$, $[C_4C_1im][BF_4]$, $[Et_3HN][CF_3SO_3]$, $[C_4im][DBP]$ and $[C_4im][BEHP]$, respectively. A special attention was paid to the region of the ν(OH) stretching modes of water (3000 - 3800 cm^{-1}). The water content in RTILs is related to the water activity value, as it was shown previously during the sorption gravimetric analysis. $[C_4C_1im][PF_6]$ is also representative of $[C_6C_1im][PF_6]$ (no present in this study) since they present only a few structural differences (**Fig. 1**), as evidenced by the similarity of their sorption behavior (**Fig. 3**). It is important to keep in mind that the IR spectra of RTILs at the water activity of 0.95 were performed directly at the end of the water sorption experiments, while the IR spectra of RTILs equilibrated at the water activity lower than 0.95 were carried out after adding the precise amount of water in agreement with the water vapor sorption isotherms. It is also important to note that dry RTILs do not absorb in the studied region (3000 - 3800 cm^{-1}). This was confirmed by the heating of studied RTILs above 80 °C to remove any residual water.

In the case of $[C_4C_1im][PF_6]$, the inset in **Fig. 5** shows two distinct bands corresponding to the ν_3 and ν_1 modes of water at 3671 and 3596 cm^{-1}, respectively. The heating of $[C_4C_1im][PF_6]$ at 65-80 °C results in the disappearance of these bands. The intensity of these water bands increases with the water content sorbed into $[C_4C_1im][PF_6]$. However, the intensity at the water activity a = 0.95 is very low compared to that found for other RTILs (it will be shown below), because $[C_4C_1im][PF_6]$ is a water-immiscible RTIL. It can be seen that the positions of the ν_3 and ν_1 bands and their shape do not change significantly as a function of the water content in $[C_4C_1im][PF_6]$. They do not change also with the physical state of water added to $[C_4C_1im][PF_6]$ (*i.e.* the water vapor or the liquid water for a = 0.60 and a = 0.95, respectively). This can indicate that the water state in $[C_4C_1im][PF_6]$ is dependent neither on the water content (which is very low) nor on the driving force induced by the water concentration gradient. On the other hand, the position and shape of the ν_3 and ν_1 bands of water dissolved in $[C_4C_1im][PF_6]$ demonstrate that the water molecules are not associated into the clusters. Thus, these water molecules can be assigned as "free" water molecules interacting *via* H-bonding with the $[PF_6]$ anion. According to many studies such as Cammarata et al.[30], Singh et al.[49], Wang et al.[35] and Danten et al.[51], in the case when water is present in small concentration and in the form of "free" water molecules in RTILs (such as $[C_4C_1im][PF_6]$ and $[C_4C_1im][BF_4]$), it interacts *via* H-bonds with the anions forming a symmetric complex: anion...H–O–H...anion. At this stage of discussion, we can say that most of the water molecules sorbed in $[C_4C_1im][PF_6]$ exist in the symmetric 1:2 type H-bonded complex: $[PF_6]$...H–O–H...$[PF_6]$. In addition to the ν_3 and ν_1 bands, a broad band of low intensity appeared around 3455

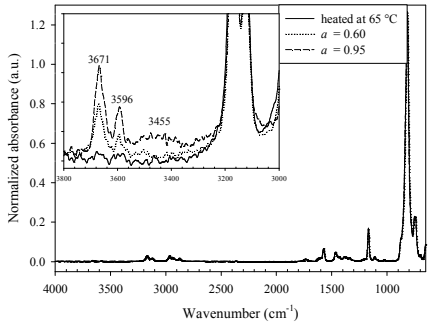

Fig. 5. ATR-IR spectra of $[C_4C_1im][PF_6]$ as a function of the water content. Inset shows the region of the ν(O–H) stretching modes of water (3000–3800 cm^{-1}).

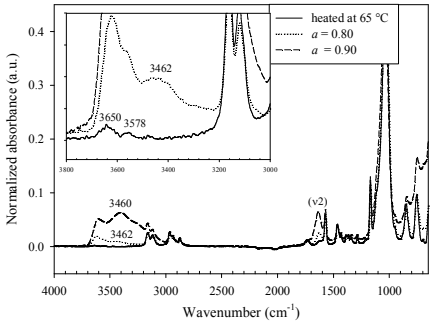

Fig. 6. ATR-IR spectra of $[C_4C_1im][BF_4]$ as a function of the water content. Inset shows the region of the ν(O–H) stretching modes of water (3000–3800 cm^{-1}).

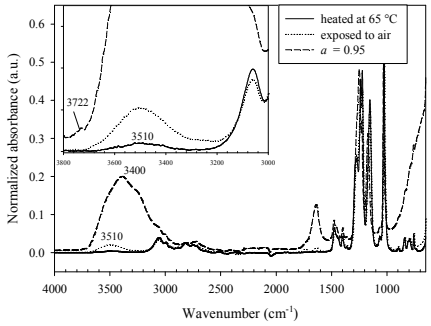

Fig. 7. ATR-IR spectra of $[Et_3HN][CF_3SO_3]$ as a function of the water content. Inset shows the region of the ν(O–H) stretching modes of water (3000-3800 cm^{-1}).

cm^{-1} at the very high water activity (a = 0.95) (**Fig. 5**). This band may correspond to a very negligible amount of the water molecules associated by the hydrogen bonds in $[C_4C_1im][PF_6]$[30,31], as evidenced by the low K_a and n values (**Table 2**).

Fig. 6 shows that after heating at 65 °C the ν_3 and ν_1 bands of very low intensity are still visible at 3650 and 3578 cm^{-1} in the case of $[C_4C_1im][BF_4]$. However, the heating of this RTIL up to 80 °C resulted in the disappearance of these bands (not shown). It means that it is necessary to dry RTILs at the temperature above 80 °C prior to measurements. The position and shape of the ν_3 and ν_1 bands of water in heated $[C_4C_1im][BF_4]$ indicate that the water molecules (in very small quantities) are in free state and, thus, may interact with the $[BF_4]$ anion forming a symmetric complex[30,31,49,51]: $[BF_4]$...H–O–H...$[BF_4]$. As stated above, these two bands (ν_3 and ν_1) are very sensitive to the water environment, that explains the different positions of ν_3 and ν_1 for $[C_4C_1im][PF_6]$ (**Fig. 5**) and $[C_4C_1im][BF_4]$ (**Fig. 6**). Moreover, the intensity of these bands after heating at 65 °C is of the same order as that in the case of $[C_4C_1im][PF_6]$ at the activity a = 0.95 (**Fig. 5**). This again proves the difference of these RTILs in terms of the water miscibility. The increase in the water content (a = 0.8) in $[C_4C_1im][BF_4]$ (**Fig. 6**) leads to the increase of the intensity of the ν_3 and ν_1 bands and their further overlapping. At the same time, a broad band of certain intensity that appeared at 3462 cm^{-1} indicates the association between the water molecules by the hydrogen bonds[30,31,49]. Moreover, the water molecules start to form the hydrodynamic shells around the RTIL ions (predominantly the anions), *i.e.* the end of the symmetric complex is observed, as evidenced by Mäki-Arvela et al.[66]. Singh et al.[49] studied the cation–anion–water interactions in the aqueous solutions of $[C_4C_1im][BF_4]$, $[C_8C_1im][Cl]$, $[C_4C_1im][CH_3OSO_3]$ and $[C_4C_1im][C_8H_{17}OSO_3]$ over the whole composition range. They found that the strong broad band in the region around 3400 - 3800 cm^{-1} was related to the absence of the anion...H–O–H...anion complexation. It was noted that the absence of such symmetric complexation in these systems was due to the existence of the water molecules in the anion hydration shells. A difference in the shape of the ν_3 and ν_1 bands is observed between the IR spectra measured for a = 0.8 and a = 0.9 (**Fig. 6**). The intensity of the broad band at 3462 cm^{-1} in $[C_4C_1im][BF_4]$ increases greatly with the water content exceeding the intensity of the ν_3 and ν_1 bands whose intensities also increase. The hydrogen bond network is strengthened with the water content increase inside $[C_4C_1im][BF_4]$. Besides, the positions of ν_3, ν_1 and the broad band at 3462 cm^{-1} slightly shift towards the lower wavenumbers region, namely to 3420 cm^{-1} for the broad and intense band, with the increase of the water activity. According to Bergstrom et al.[67], the broad band in the region around 3400 cm^{-1} may be attributed to the water molecules interacting strongly with the anion and to the water molecules forming aggregates around this anion. All these data indicate the formation of the water aggregates or other types of the water association in $[C_4C_1im][BF_4]$ at the high activity (a = 0.95). The presence of the water clusters are observed in the aqueous mixtures of $[C_4C_1im][BF_4]$ using NMR and the molecular dynamics simulation studies[68]. Thus, the $[BF_4]$ anion, unlike the $[PF_6]$ anion, shows the behavior of an anion of a strong basicity (the same goes for the other anions as will be shown below). One can conclude that the molecular state of water depends on the water content in $[C_4C_1im][BF_4]$: when the water content increases, the water molecules (that are free at the low water content) become closer to each other and start to associate by the hydrogen bonds (formation of H-bond network) up to the creation of the threshold for the water clustering. This threshold is usually called the critical concentration. As the water molecular state depends strongly on

the water concentration in $[C_4C_1im][BF_4]$, the FTIR measurements of $[C_4C_1im][BF_4]$ with the liquid water were performed (not shown). The obtained results are in good agreement with the gravimetric analysis results proving that the water molecules have strong interactions with $[C_4C_1im][BF_4]$ and have a facility of the clustering formation at the high activity. The same observation was done in the literature thus qualifying $[C_4C_1im][BF_4]$ as water-miscible RTIL[30,31,49,51].

$[Et_3HN][CF_3SO_3]$ was either heated at 65 °C or exposed to the humidity of ambient air (*ca.* 65 - 75% in our experiments). In both cases a broad band of water around 3510 cm^{-1} was revealed (**Fig. 7**). The intensity of this band significantly increases after the exposition to air characterizing $[Et_3HN][CF_3SO_3]$ as very hygroscopic RTIL. The shape and position of this band indicate that it results from the overlapping of the ν_3 and ν_1 bands due to the water intermolecular forces[30,31,49]. The water molecules in $[Et_3HN][CF_3SO_3]$ would not be "free" at the low water content. Unlike $[C_4C_1im][BF_4]$ and $[C_4C_1im][PF_6]$, it appears that the water molecules sorbed in $[Et_3HN][CF_3SO_3]$ can form a hydrogen bond network even at the low activity and can strongly surround the $[CF_3SO_3]$ anions (probably in the hydrodynamic shells). This is not surprising as $[Et_3HN][CF_3SO_3]$ reveals very strong interactions with the water molecules as shown previously (**Fig. 3**). $[CF_3SO_3]$ is an anion with a very strong basicity. At the high water content (a = 0.95), the intensity and width of the water band strongly increase, thus strengthening the H-bond network. The intensity of this band is the highest in the present study, that corresponds to the highest water uptake observed from the water sorption isotherm at a = 0.95 (2.03 g-water/g-$[Et_3HN][CF_3SO_3]$). Besides, the shift of this band to the lower wavenumbers (exactly to 3400 cm^{-1}) is characteristic to the liquid-like water state. This indicates a strong presence of the water clusters or water aggregates in $[Et_3HN][CF_3SO_3]$[30]. On the other hand, the shape of the band remains essentially unchanged with the water content increase testifying that although the state of water differs from that in $[C_4C_1im][BF_4]$ and $[C_4C_1im][PF_6]$ it does not change as a function of the water concentration. It was possible to detect a weak band at *ca.* 3722 cm^{-1} at a = 0.95 (**Fig. 7**) which can be assigned to the water molecules weakly bounded to the CF_3 anion groups[30]. In conclusion, one can say that in the case of $[Et_3HN][CF_3SO_3]$ the water molecules, firmly associated by the hydrogen bonds even at the low water activity, start to strongly aggregate when the water content reaches the critical concentration[30,31,49].

In the case of $[C_4im][DBP]$ (**Fig. 8**) and $[C_4im][BEHP]$ (**Fig. 9**), a broad band of water appears at 3410 and 3402 cm^{-1}, respectively. In both cases, this band results from the overlapping of the ν_3 and ν_1 bands. The shape and the position of the band indicate that the water molecules sorbed in $[C_4im][DBP]$ and $[C_4im][BEHP]$ (at their respective activity levels) are self-associated in the H-bond network and that the hydrodynamic shells are probably formed with the [DBP] and [BEHP] anions. Although $[C_4im][DBP]$ and $[C_4im][BEHP]$ were not equilibrated at the same activity (0.20 and 0.60, respectively), the magnitude of the band of water is of the same order in both cases. This fact testifies that $[C_4im][DBP]$ absorbs more water molecules than $[C_4im][BEHP]$ or, in other words, the

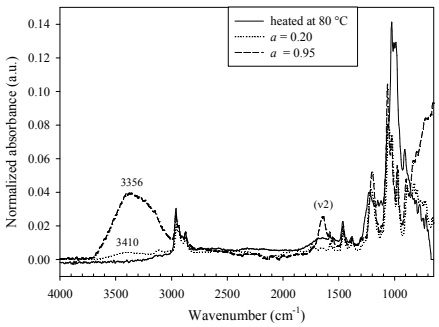

Fig. 8. ATR-IR spectra of $[C_4im][DBP]$ as a function of the water content.

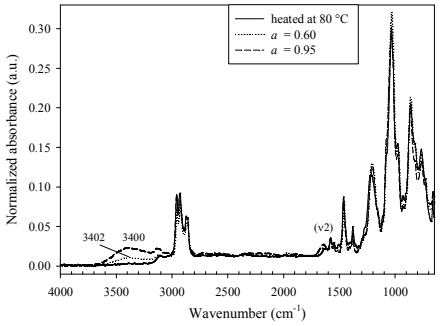

Fig. 9. ATR-IR spectra of $[C_4im][BEHP]$ as a function of the water content.

[DBP] anion is more basic than the [BEHP] one. At the high water content (a = 0.95), the intensity of the band of water increases in both these RTILs. Thus, one may suppose that the H-bond network is further strengthened over the water content. The intensity increase is little more important in the case of $[C_4im][DBP]$ (**Fig. 8**) than in the case of $[C_4im][BEHP]$ (**Fig. 9**), indicating a strong presence of the water aggregates or other types of the water association in $[C_4im][DBP]$. We note also the slight shift of the water band towards the lower wavenumbers in the case of $[C_4im][DBP]$ (3356 cm^{-1}). On the other hand, the shape of the band of water in both cases does not really change with the water activity and also with the physical state of water added to RTILs (*i.e.* the liquid water and the water vapor). This means that the molecular state of water in these RTILs seems to be independent on both their water concentration and the physical state of added water. So, the water molecules are strongly associated by H-bonds in $[C_4im][DBP]$ and $[C_4im][BEHP]$ at the low water activity and easily aggregate when the water content reaches the critical concentration. All these results are in agreement with the gravimetric analysis which demonstrates that $[C_4im][BEHP]$ is a little less water miscible compared to $[C_4im][DBP]$ and, consequently, $[C_4im][DBP]$ presents more water aggregates at the high water activity.

As seen from this article, the preferred sites of interaction with the water molecules are the RTIL anions. The water molecules interact with the anions by the hydrogen bonds forming either the symmetric 1:2 type H-bonded complexes or the hydrodynamic

shells. Therefore, the environment of the anions changes in the presence of water. Consequently, the shape of the IR band of anions changes slightly due to the presence of water close to the anion[30,31,49]. No noticeable change is observed for the band of the $[PF_6]$ anion at 816 cm^{-1} (in $[C_4C_1im][PF_6]$) whatever the water concentration (**Fig. 10a**), while the band of the $[BF_4]$ anion at 1035 cm^{-1} (in $[C_4C_1im][BF_4]$) slightly shifts to the higher wavenumbers (**Fig. 10b**). However, the position of the $[CF_3SO_3]$ anion band depends on the water activity (**Fig. 10c**). In the case of $[C_4im][DBP]$ and $[C_4im][BEHP]$, this effect is visible over a large part of the ATR-IR spectra because their anions have a complex structure.

Conclusions

The water sorption properties of six RTILs ($[C_4C_1im][BF_4]$, $[C_4C_1im][PF_6]$, $[C_6C_1im][PF_6]$, $[C_4im][DBP]$, $[C_4im][BEHP]$ and $[Et_3HN][CF_3SO_3]$) were studied over the whole range of water activity. The experimental data of all water sorption isotherms (of type III) were well fitted with the dual mode (Henry-clustering) and the NRTL models. The mass uptake is in fact linear and non-specific at the low and intermediate water activity and then curve upward. The RTIL water uptake increases in the following order (up to a = 0.8): $[C_6C_1im][PF_6] \leq [C_4C_1im][PF_6] < [C_4C_1im][BF_4] \approx [C_4im][BEHP] < [Et_3HN][CF_3SO_3] \leq [C_4im][DBP]$. $[C_6C_1im][PF_6]$ and $[C_4C_1im][PF_6]$, qualified as water-immiscible RTILs, show the lowest water uptakes, while $[C_4C_1im][BF_4]$ and $[C_4im][BEHP]$ and especially $[C_4im][DBP]$ and $[Et_3HN][CF_3SO_3]$ show the strongest water uptakes. The water miscibility is found to be linked with the anion nature, and increases in the following order: $[PF_6] < [BF_4] \approx [BEHP] < [DBP] < [CF_3SO_3]$ (for the same cation). The anion interacts with water by the hydrogen bonds and, at the same time, promotes the formation of the hydrogen bond network between the water molecules. The cation nature has also an effect on the water sorption of RTILs, which increases in the following order: $[C_6C_1im] \leq [C_4C_1im] \leq [C_4im] < [Et_3HN]$ (for the same anion). However, the cation effect remains secondary compared to that of the anion. At the high activity (a > 0.8), the water uptake increases strongly in RTILs based on the anion with a strong basicity ($[BF_4]$, $[DBP]$ and especially $[CF_3SO_3]$), as the water molecules become closer to each other and the H-bond network is further strengthened. Consequently, the water molecules sorbed in these RTILs form aggregates or, perhaps, even droplets of the bulk liquid-like water at the high activity.

The results of the RTIL sorption measurements were linked to the molecular state of water dissolved in RTILs studied by the infrared spectroscopy. The water molecules dissolved in $[C_4C_1im][PF_6]$ and $[C_6C_1im][PF_6]$ (water-immiscible RTILs) are found to be not self-associated whatever the water content, and can be assigned as "free" water molecules interacting *via* the H-bonding with the $[PF_6]$ anions in the symmetric complex: $[PF_6]$…HOH…$[PF_6]$. On the contrary, the water molecules sorbed in $[C_4im][DBP]$, $[C_4im][BEHP]$ and $[Et_3HN][CF_3SO_3]$ (water-miscible RTILs) are strongly associated with each other by the H-bonds and also with the anions even at the low activity, and can easily aggregate when the water content reaches the critical concentration at the high activity. Finally, $[C_4C_1im][BF_4]$ (also water-miscible RTIL) follows the same trend, except at the low activity where the water molecules are not self-associated (free water molecules) interacting *via* H-bonding with the $[BF_4]$ anions in a symmetric complex: $[BF_4]$…HOH…$[BF_4]$.

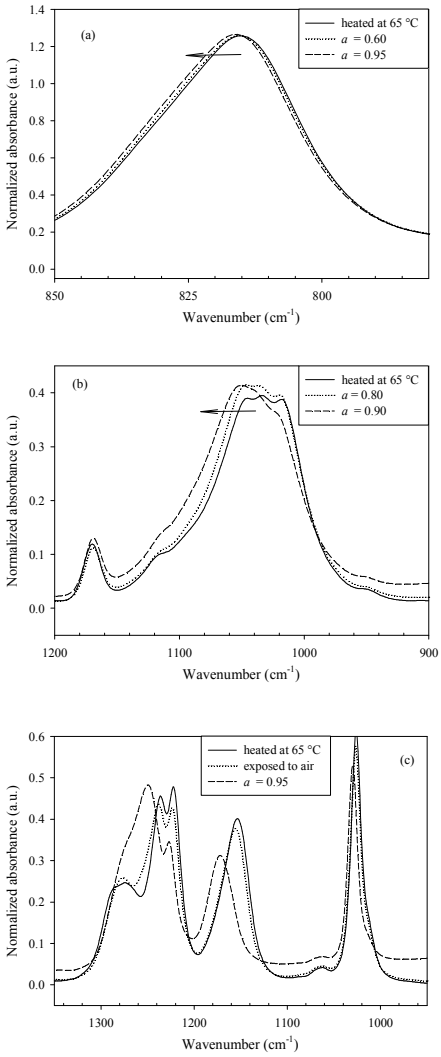

Fig. 10. ATR-IR spectra of (a) $[C_4C_1im][PF_6]$, (b) $[C_4C_1im][BF_4]$ and (c) $[Et_3HN][CF_3SO_3]$ in the $\nu(PF_6)$, the $\nu(BF_4)$ and $\nu(CF_3SO_3)$ band region, respectively.

Acknowledgements

The authors acknowledge the financial support provided by the Réseau Polymères Innovants (France). The research study was partially supported by CNRS and National Academy of Science of Ukraine (grant # VJCXC 42359).

References

1 S. Keskin, D. Kayrak-Talay, U. Akman, and O. Hortacsu, *J. Supercrit. Fluids,* 2007**, 4**, 150.
2 J. G. Huddleston, A. E. Visser, W. M. Reichert, H. D. Willauer, G. A. Broker, and R. D. Rogers, *Green Chem.,* 2001**, 3**, 156.

3 J. F. Brennecke, and E.J. Maginn, *AICHE J.,* 2001, **47**, 2384.
4 M. Freemantle, *Chem. Eng. News,* 2000, **78**, 37.
5 T. Welton, *Chem. Rev.,* 1999, **99**, 2071.
6 H. Olivier-Bourbigou, and L. Magna, *J. Molec. Cat. A - Chem.,* 2002, **182**, 419.
7 R. Sheldon, *Chem. Comm.,* 2001, **23**, 2399.
8 J. G. Huddleston, H. D. Willauer, R. P. Swatloski, A. E. Visser, and R. D. Rogers, *Chem. Comm.,* 1998, **16**, 1765.
9 R. Fortunato, C. A. M. Afonso, J. Benavente, E. Rodriguez-Castellon, and J. G. Crespo, *J. Membr. Sci.,* 2005, **256,** 216.
10 R. Fortunato, C. A. M. Afonso, M. A. M. Reis, and J. G. Crespo, *J. Membr. Sci.,* 2004, **242**, 197.
11 B. G. Wang, J. Lin, F. Wu, and Y. Peng, *Ind. Eng. Chem. Res.,* 2008, **47**, 8355.
12 P. Scovazzo, *J. Membr. Sci.,* 2010, **355**, 7.
13 L. C. Branco, J. G. Crespo, and C. A. M. Afonso, *Angewandte Chemie-Intern. Ed.,* 2002, **41,** 2771.
14 M. Matsumoto, Y. Inomoto, and K. Kondo, *J. Membr. Sci.,* 2005, **246**, 77.
15 F. J. Hernandez-Fernandez, A. P. D. Rios, F. Tomas-Alonso, D. Gomez, and G. Villora, *J. Chem. Technol. Biotechnol.,* 2009, **84**, 337.
16 A. Dahi, K. Fatyeyeva, D. Langevin, C. Chappey, S. P. Rogalsky, O. P. Tarasyuk, A. Benamor, S. Marais, *J. Membr. Sci.,* 2014, **458**, 164.
17 F. F. Krull, C. Fritzmann, and T. Melin, *J. Membr. Sci.,* 2008, **325**, 509.
18 L. A. Neves, N. Nemestothy, V. D. Alves, P. Cserjesi, K. Belafi-Bako, and I. M. Coelhoso, *Desalination,* 2009, **240**, 311.
19 P. Luis, L. A. Neves, C. A. M. Afonso, I. M. Coelhoso, J. G. Crespo, A. Garea, and A. Irabien, *Desalination,* 2009, **245,** 485.
20 S. Chun, S. V. Dzyuba, and R. A. Bartsch, *Anal. Chem.,* 2001**,** **73**, 3737.
21 F. J.Alguacil, M. Alonso, F. A. Lopez, A. Lopez-Delgado, I. Padilla, and H. Tayibi, *Chem. Eng. J.,* 2010, **157**, 366.
22 M. Armand, F. Endres, D. R. MacFarlane, H. Ohno, and B. Scrosati, *Nature Mater.,* 2009, **8**, 621.
23 C. Iojoiu, P. Judeinstein, and J.-Y. Sanchez, *Electrochim. Acta,* 2007, **53,** 1395.
24 A. Dahi, K. Fatyeyeva, D. Langevin, C. Chappey, S. P. Rogalsky, O. P. Tarasyuk, S. Marais, *Electrochim. Acta*, 2014, **130**, 830.
25 R. F. de Souza, J. C. Padilha, R. S. Goncalves, and J. Dupont, *Electrochem. Commun.,* 2003, **5**, 728.
26 J. S. Baek, J. S. Park, S. S. Sekhon, T. H. Yang, Y. G. Shul, qnd J. H. Choi, *Fuel Cells,* 2010, **10**, 762.
27 M. Doyle, S. K. Choi, and G. Proulx, *J. Electrochem. Soc.,* 2000, **147**, 34.
28 C. F. Poole, *J. Chromatogr. A,* 2004, **1037**, 49.
29 K. R. Seddon, A. Stark, and M. J. Torres, *Pure Appl. Chem.,* 2000, ***72,*** 2275.
30 L. Cammarata, S. G. Kazarian, P. A. Salter, and T. Welton, *Phys. Chem. Chem. Phys.,* 2001, **3**, 5192.
31 J. M. Andanson, F. Jutz, and A. Baiker, *J. Phys. Chem. B,* 2010, **114**, 2111.
32 J. S. Wilkes, and M. J. Zaworotko, *J. Chem. Soc. - Chem. Commun.,* 1992, **13**, 965.
33 C. D. Tran, S. H. D. Lacerda, and D. Oliveira, *Appl. Spectroscopy,* 2003, ***57***, 152.
34 J. L. Anthony, E. J. Maginn, and J. F. Brennecke, *J. Phys. Chem. B,* 2001, **105**, 10942.
35 Y. Wang, H. Li, and S. A. Han, *J. Phys. Chem. B,* 2006, **110,** 24646.
36 K. R. Seddon, and A. Stark, *Green Chem.,* 2002, **4**, 119.
37 R. P. Swatloski, J. D. Holbrey, and R. D. Rogers, *Green Chem.,* 2003, **5**, 361.
38 B. Yoon, C. H. Yen, S. Mekki, S. Wherland, and C. M. Wai, *Ind. Eng. Chem. Res.,* 2006, **45**, 4433.
39 R. Fortunato, M. J. Gonzalez-Munoz, M. Kubasiewicz, S. Luque, J. R. Alvarez, C. A. M. Afonso, I. M. Coelhoso, and J. G. Crespo, *J. Membr. Sci.,* 2005, **249,** 153.
40 R. A. Brown, P. Pollet, E. McKoon, C. A. Eckert, C. L. Liotta, and P. G. Jessop, *J. Am. Chem. Soc.,* 2001, **123,** 1254.
41 A. G. Fadeev, and M. M. Meagher, *Chem. Comm.,* 2001, **3,** 295.
42 A. E. Visser, R. P. Swatloski, W. M. Reischert, R. Mayton, S. Sheff, A. Wierzbicki, J. H. Davis, and R. D. Rogers, *Environ. Sci. Technol.,* 2002, **36**, 2523.
43 K. Fujita, D. R. MacFarlane, and M. Forsyth, *Chem. Comm.,* 2005, 4804.
44 W. Zhao, G. He, L. Zhang, J. Ju, H. Dou, F. Nie, C. Li, and H. Liu, *J. Membr. Sci.,* 2010, **350**, 279.
45 Y. Cao, Y. Chen, X. Sun, Z. Zhang, and T. Mu, *Phys. Chem. Chem. Phys.,* 2012, **14**, 12252.
46 Y. Cao, Y. Chen, L. Lu, Z. Xue, and T. Mu, *Ind. Eng. Chem. Res.,* 2013, **52**, 22073.
47 R. Ludwig, *Angew. Chem. Int. Ed.,* 2001, **40**, 1808.
48 L. F. Scatena, M. G. Brown, and G. L. Richmond, *Science,* 2001, **292**, 908.
49 T. Singh, and A. Kumar, *Vibr. Spectroscopy.,* 2011, **55**, 119-125.
50 Y. Chen, Y. Cao, Y. Zhang, and T. Mu, *J. Mol. Structr.,* 2014, **1058,** 244.
51 Y. Danten, M. I. Cabaço, and M. Besnard, *J. Mol. Liq.,* 2010**,** **153**, 57.
52 J.-Y. Sanchez, C. Iojoiu, J.-C. Leprêtre, M. Martinez, M. Hanna, L. Cointeaux, Y. Molmeret, N. El Kissi, P. Judeinstein, D. Langevin, and R. Mercier, *Amer. Chem. Soc., Div. Fuel Chem.,* 2010, **55**, 117.
53 A.-L. Revelli, F. Mutelet, and J.-N. Jaubert, *J. Chem. Thermodyn.,* 2010, **42,** 177.
54 L. S. Belvèze, Thesis, University of Notre Dame, Indiana, 2004.
55 A. Jonquières, L. Perrin, A. Durand, S. Arnold, and P. Lochon, *J. Membr. Sci.,* 1998, **147**, 59.
56 G. S. Park, *Transport principles–solution, diffusion and permeation in polymer membranes*. in: Bungay P.M., et al. (Eds.), Synthetic Membranes: Science, Engineering & Applications, Reidel, Holland, 1986, pp 57.
57 A. M. O'Mahony, D. S. Silvester, L. Aldous, C. Hardacre, and R. G. Compton, *J. Chem. Eng. Data,* 2008, **53**, 2884.
58 Y. Peng, J. Fu, and X. Lu, *Fluid Phase Equilibr.,* 2014, **363**, 220.
59 J. Zhao, C.-X. Li, and Z.-H. Wang, *J. Chem. Eng. Data,* 2006, **51**, 1755.
60 K. Fujita, D. R. MacFarlane, M. Forsyth, M. Yoshizawa-Fujita, K. Murata, N. Nakamura, and H. Ohno, *Biomacromolecules,* 2007, **8**, 2080.
61 A. Richardt, C. Mrestani-Klaus, and F. Bordusa, *J. Mol. Liq.,* 2014, **192**, 9.
62 J.-F. Wang, C.-X. Li, Z.-H. Wang, Z.-J. Li, and Y.-B. Jiang, *Fluid Phase Equilibr.,* 2007, **255**, 186.
63 I. Jureviciute, S. Bruckenstein, and A. R. Hillman, *J. Electroanal. Chem.,* 2000, **488**, 73.
64 E. Zoidis, J. Yarwood, T. Tassaing, Y. Danten, and M. Besnard, *J. Mol. Liq.,* 1995, **64**, 197.
65 H. Kusanagi, and S. Yukawa, *Polymer,* 1994, **35**, 5637.
66 P. Mäki-Arvela, I. Anugwom, P. Virtanen, R. Sjöholm, and J. P. Mikkola, *Ind. Crops Products,* 2010, **32**, 175.
67 P. A. Bergstroem, J. Lindgren, and O. Kristiansson, *J. Phys. Chem.,* 1991, **95**, 8575.
68 M. Moreno, F. Castiglione, A. Mele, C. Pasqui, and G. Raos, *J. Phys. Chem. B,* 2008, **112,** 7826.